Article

pubs.acs.org/Biomac

Surface-Functionalization of Nanostructured Cellulose Aerogels by Solid State Eumelanin Coating

Lucia Panzella,[*,†] Lucio Melone,[‡,§,∥] Alessandro Pezzella,[†] Bianca Rossi,[‡,§] Nadia Pastori,[‡,§] Marco Perfetti,[†,⊥] Gerardino D'Errico,[†,⊥] Carlo Punta,[*,‡,§] and Marco d'Ischia[†]

[†]Department of Chemical Sciences, University of Naples "Federico II", Complesso Universitario Monte S.Angelo, via Cintia 4, I-80126 Naples, Italy

[‡]Department of Chemistry, Materials, and Chemical Engineering "G. Natta", Politecnico di Milano, Via Mancinelli 7, I-20131 Milano, Italy

[§]INSTM, National Consortium of Materials Science and Technology, Local Unit Politecnico di Milano, Piazza Leonardo da Vinci 32, I-20133 Milan, Italy

[∥]Università degli studi e-Campus, Via Isimbardi 10, I-22060 Novedrate, Como, Italy

[⊥]CSGI (Consorzio per lo Sviluppo dei Sistemi a Grande Interfase), Florence, Italy

Supporting Information

ABSTRACT: Bioinspired aerogel functionalization by surface modification and coating is in high demand for biomedical and technological applications. In this paper, we report an expedient three-step entry to all-natural surface-functionalized nanostructured aerogels based on (a) TEMPO/NaClO promoted synthesis of cellulose nanofibers (TOCNF); (b) freeze-drying for aerogel preparation; and (c) surface coating with a eumelanin thin film by ammonia-induced solid state polymerization (AISSP) of 5,6-dihydroxyindole (DHI) or 5,6-dihydroxyindole-2-carboxylic acid (DHICA) previously deposited from an organic solution. Scanning electron microscopy showed uniform deposition of the dark eumelanin coating on the template surface without affecting porosity, whereas solid state ^{13}C NMR and electron paramagnetic resonance (EPR) spectroscopy confirmed the eumelanin-type character of the coatings. DHI melanin coating was found to confer to TOCNF templates a potent antioxidant activity, as tested by the 2,2-diphenyl-1-picrylhydrazyl (DPPH) and 2,2′-azinobis(3-ethylbenzothiazoline-6-sulfonic acid) (ABTS) assays as well as strong dye adsorption capacity, as tested on methylene blue. The unprecedented combination of nanostructured cellulose and eumelanin thin films disclosed herein implements an original all-natural multifunctional aerogel biomaterial realized via an innovative coating methodology.

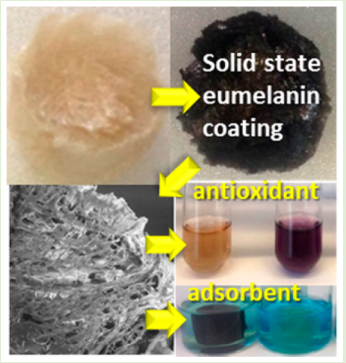

INTRODUCTION

Aerogels are cellular solids usually obtained by the random interconnection of nanoparticles or nanowires.[1] The resulting network skeleton provides ultralightweight highly porous materials, which have attracted increasing interest in the last years for their potential ranging applications as drug-carriers, catalyst supports, thermal and acoustic insulators, adsorbent units, and templates for active coating.[2,3] Both inorganic and organic solutions have been proposed in this field, the latter usually affording better performances from a mechanical strength point of view.[4−6] Moreover, recent environmental issues and the creation of recycle-based and sustainable societies have driven the fundamental research and application of materials deriving from natural and recycled sources.

In this context, cellulose and nanocellulose have been widely investigated for the fabrication of aerogels and membranes, following different homogeneous and heterogeneous approaches.[7] The choice of this biopolymer allows to take advantage of the enhanced chemical-physical properties of the polysaccharide, providing, at the same time, biodegradable and eco-friendly materials, which match the common rules of green chemistry. In particular, nanofibrillated cellulose has been successfully suggested as a building block for the construction of aerogel skeletons, due to the low density, high strength and large surface area of the fibers.[8−10]

Among the several techniques suggested for cleaving the hierarchically ordered native cellulose, (2,2,6,6-tetramethylpiperidin-1-yl)oxyl (TEMPO)-mediated oxidation appears to be the first choice for the production of cellulose nanofibers (CNF), due to the simplicity, efficiency, and versatility of the approach, which is performed under mild conditions (room temperature) and with inexpensive reagents.[11−13] Corresponding aerogels can be obtained following a simple reported procedure, consisting in the freeze-drying processing of the milky suspension of TEMPO-oxidized CNF (TOCNF).[14,15]

Received: November 6, 2015
Revised: December 22, 2015

DOI: 10.1021/acs.biomac.5b01497
Biomacromolecules XXXX, XXX, XXX−XXX

While interesting by themselves as biocompatible organic substrates to be used either as drug delivery vehicles or as scaffolds for tissue engineering,[16−18] CNF-aerogels can also be further manipulated in order to confer or optimize functionality. A possible approach consists in promoting nanofibers reticulation by formulating the aerogel in the presence of suitable cross-linkers. The latter usually have the dual function of consolidating the network by cross-linking of nanofibers and of introducing new functional groups with specific activity.[19,20] In this context, we have recently reported the synthesis of adsorbent materials with sponge-like structure by cross-linking TOCNF with branched polyethylenimine (bPEI). The resulting nanostructured sponges have been proposed as efficient adsorbent materials for water remediation.[21] Moreover, we have extended this protocol to the preparation of novel polymeric conjugate materials, with a porous structure, which were successfully used for the heterogeneous sensing of fluoride anions in DMSO solution.[22]

Alternative approaches involve use of CNF-aerogels as templates for either inorganic or organic coatings.[23−27]

A highly attractive, yet still apparently unexplored entry to CNF functionalization would be based on the exploitation of the unique physicochemical properties of eumelanins,[28−32] the antioxidant and photoprotective pigments of human skin and eyes. Eumelanins are insoluble biopolymers derived biogenetically from tyrosine or DOPA via the oxidative polymerization of 5,6-dihydroxyindole (DHI) and 5,6-dihydroxyindole-2-carboxylic acid (DHICA; Figure 1). Both natural eumelanins

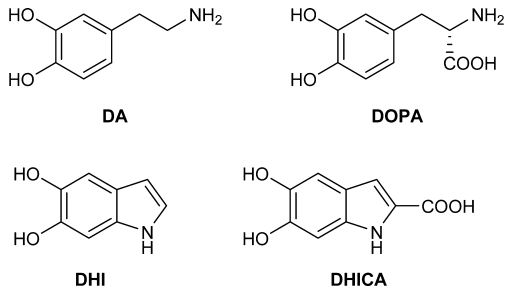

Figure 1. Chemical structure of principal melanin precursors.

and their synthetic mimics are endowed with a unique set of physicochemical properties, including a broadband absorption spectrum unusual for organic pigments, semiconductor-like behavior, a stable free radical character, efficient UV-dissipation and, notably, antioxidant and free radical scavenging properties, suggesting application in organic electronic, biosensing, nanomedicine, and drug delivery.[33] A mussel-inspired variant of eumelanin biopolymers produced by autoxidation of the catecholamine dopamine (DA) leads to the formation of the black polydopamine (PDA), a versatile biomaterial widely employed for the deposition of films or multifunctional coatings on a wide range of materials.[34−39]

In this context, in order to develop an efficient nanostructured system for drug delivery, we envisioned that the design of an all-natural multifunctional biomaterial by PDA antioxidant coating of CNF aerogels could provide three additional valuable properties to the cellular solid: (i) a drastically reduced cytotoxicity, due to the enhanced antioxidant activity obtained by mimicking Nature's strategies for controlling and harnessing biooxidation processes; (ii) a higher stability in water, due to the hydrophobic coating; and (iii) a remarkable adsorption efficiency, useful for loading of target molecules.

PDA coating of nonoxidized cellulose microfibrillated membranes was reported recently together with the efficient performance of the new material as separator for lithium-ion batteries.[40] However, the PDA-based dip coating technology was unsuitable for application to CNF due to the limited resistance of the latter to degradation in aqueous media, requiring development of alternate procedures.

An alternative route for eumelanin coating has been proposed recently,[41] which allows to overcome the main issues associated with the limited processability of eumelanins due to insolubility in most solvents. Typically, eumelanin thin films are obtained by direct deposition of the pigment from aqueous alkali favoring partial solubilization due to oxidative backbone modification. In the ammonia-induced solid state polymerization (AISSP) protocol, a soluble eumelanin monomer is uniformly deposited on the substrate from an organic solvent and is then exposed to gaseous ammonia in air-equilibrated atmosphere. Under these conditions, the monomer undergoes polymerization in the absence of solvent with apparent darkening denoting formation of eumelanin film capable of reproducing the shape of underlying substrates. As monomer precursors, DHI and DHICA can be selected in place of the commonly used DA or DOPA for melanin-coating due to their solubility in organic solvents, higher oxidizability, and the superior antioxidant properties of DHI and DHICA melanins.[32,42−46]

Herein we report AISSP-based eumelanin coating as a viable biomimetic strategy to confer antioxidant and adsorption properties to TOCNF aerogels in organic media. Salient outcomes of the study include (a) the extension of the solid-state polymerization protocol for eumelanin coating to porous CNF aerogels, (b) the characterization of the antioxidant and paramagnetic properties of the first all-natural bioinspired organic aerogel coated with a multifunctional bioinspired eumelanin layer, and (c) the dependence of eumelanin coating properties on the monomer used.

MATERIALS AND METHODS

Materials. 5,6-Dihydroxyindole (DHI) and 5,6-dihydroxyindole-2-carboxylic acid (DHICA) were prepared according to a reported procedure.[47] All other chemicals were commercially available and were used without further purification.

Synthetic Procedures. *Synthesis of TOCNF Aerogels.* TOCNF were obtained according to the procedure reported in our previous paper.[21,27] Briefly, KBr (1.19 g, 10.0 mmol) and TEMPO (156 mg, 1 mmol) were dissolved in deionized water (450 mL) in a three-necked, round-bottom flask. Cotton wool (8.1 g, 50.0 mmol of anhydroglucose) was added to the solution and soaked for 1 h at room temperature, after which a 12.5% w/w sodium hypochlorite solution (36 mL) was added. The pH value was maintained in the range of 10.5−11 by using 0.5 M aqueous sodium hydroxide solution. The obtained suspension was stirred for 6 h. The cellulose fibers were then collected by filtration onto a sintered glass funnel, washed with deionized water (250 mL, 3×), and redispersed in water at pH 11.0 (200 mL). The slurry was sonicated at 0 °C using a Branson Sonifier 250 equipped with a 6.5 mm probe tip working at 20 kHz in continuous mode, with an output power 50% the nominal value (200 W), until an almost transparent liquid was obtained (approximately 1 h of sonication). After acidification (to pH 1−2) with concentrated HCl (37% w/w aqueous solution), the white precipitate was recovered on a sintered glass funnel and washed extensively with deionized water (6 × 200 mL). The precipitate was redispersed in water in the presence of $NH_4OH_{(aq)}$ in order to obtain a white slurry (160 mL) at

DOI: 10.1021/acs.biomac.5b01497
Biomacromolecules XXXX, XXX, XXX−XXX

Scheme 1. Protocol for the Synthesis of TOCNF

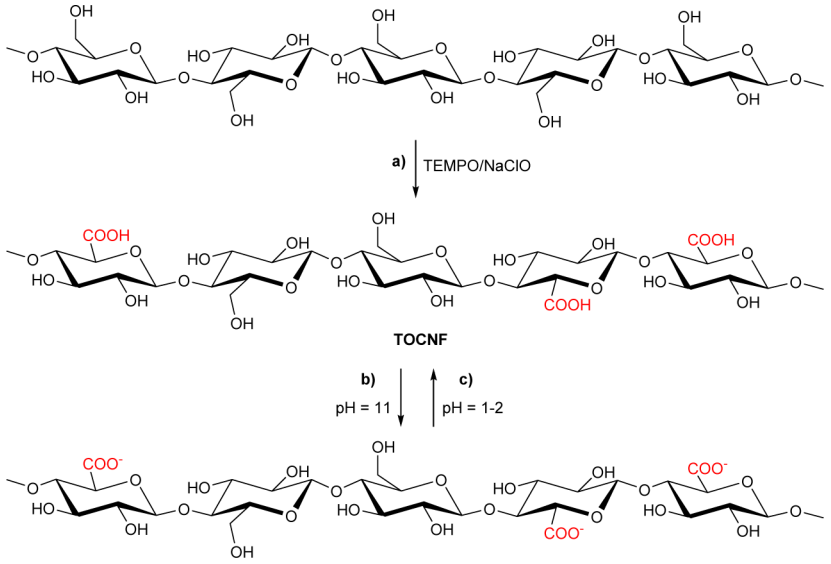

pH 11 and containing 3.5% w/v of dry CNF. This was stirred for 1 h and then sonicated for 30 min in an ice bath before being pipetted into 24-well plates (10 mL in each well) and frozen at −80 °C for 12 h. The freeze-drying at −60 °C for 48 h afforded white cylindrical CNF aerogels.

Preparation of Melanin-Coated TOCNF (Mel-TOCNF) Aerogels by Ammonia-Induced Solid State Polymerization (AISSP). The circular disks of CNF aerogels were dipped into a 1 mg mL^{-1} DHI or DHICA solution in ethyl acetate (or ethyl acetate alone for the blank) and exposed for 3 h to air-equilibrated gaseous ammonia from an ammonia solution (28% in water) in a sealed camera at 1 atm pressure and 25 °C. Mel-CNF and blank-CNF aerogels were then dried under vacuum for 3 h. For preparation of DHI and DHICA melanin a 1 mg mL^{-1} ethyl acetate solution of each substrate was exposed to gaseous ammonia as above and after 3 h taken to dryness to recover the dark brown pigments.

Characterization. The ^{13}C cross-polarization magic-angle-spinning (CP-MAS) spectra were recorded with an FT-NMR AvanceTM 500 (Bruker BioSpin S.r.l) with a superconducting ultrashield magnet of 11.7 T operating at 125.76 MHz ^{13}C frequency. The following conditions were applied: repetition time 4 s, ^{1}H 90 pulse length 4.0 ms, contact time 1.2 ms, and spin rate 8 kHz. The compounds were placed in a zirconium rotor, 4 mm in diameter and 18 mm high. The chemical shifts were recorded relative to glycine standard, previously acquired (C═O signal: 176.03 ppm, relative to tetramethylsilane reference).

Scanning electron microscopy (SEM) was performed using a variable-pressure instrument (SEM Cambridge Stereoscan 360) at 100/120 Pa with a detector VPSE. The operating voltage was 20 kV with an electron beam current intensity of 150 pA. The focal distance was 8 mm. The specimens were used without any treatment. The SEM images were obtained from cryo-sectioned samples.

Electron paramagnetic resonance (EPR) measurements were performed by following an experimental procedure recently set up for paraffin-embedded sections of melanoma samples[48] and used in the characterization of DHI and DHICA melanins.[32] Samples were measured using an X-band (9 GHz) Bruker Elexys E-500 spectrometer (Bruker, Rheinstetten, Germany), equipped with a superhigh sensitivity probe head. DHI Mel-TOCNF and DHICA Mel-TOCNF samples were transferred to flame-sealed glass capillaries which, in turn, were coaxially inserted in a standard 4 mm quartz sample tube. DHI and DHICA melanins obtained by the same preparation protocol were also investigated as references. Measurements were performed at room temperature. The instrumental settings were as follows: sweep width, 100 G; resolution, 1024 points; modulation frequency, 100 kHz; modulation amplitude, 2.0 G. The amplitude of the field modulation was preventively checked to be low enough to avoid detectable signal overmodulation. EPR spectra were measured with a microwave power of ∼4 mW to avoid microwave saturation of resonance absorption curve. A total of 64 scans were accumulated to improve the signal-to-noise ratio. For power saturation experiments, the microwave power was gradually incremented from 0.004 to 64 mW. The g value and the spin density were evaluated by means of an internal standard, Mn^{2+}-doped MgO, prepared by modifying a synthesis protocol reported in literature.[49] Since sample hydration was not controlled during the measurements, spin density values have to be considered as order of magnitude estimates.[46]

Water contact angle (WCA) was measured with a Data Physics OCA150 contact angle system at ambient humidity and temperature, and the software was SCA20 version 2.3.9 build 46. Droplets of deionized water were placed at different locations on the aerogel samples with a microsyringe. The droplet volume was 8 μL. A minimum of five readings were taken for each sample in order to determine the average values. Typical standard deviations are 2−3°.

The bulk density of the TOCNF and Mel-TOCNF aerogels was determined from the dimensions and weights of the samples, while the related porosity (P) was calculated using the bulk density of the aerogels (d_b) and the density of the crystalline cellulose nanofibers (d_n = ∼1.6 g cm^{-3}) using eq 1, which is obtained from the simple mixing rule with a negligible gas density.[50]

$$P(\%) = 100\left(1 - \frac{d_b}{d_n}\right) \quad (1)$$

Antioxidant Experiments. *2,2-Diphenyl-1-picrylhydrazyl (DPPH) Assay.*[51,52] Mel-TOCNF or blank TOCNF aerogels were finely cut with scissors and suspended at 0.5−2 mg mL^{-1} in a freshly prepared 0.2 mM solution of DPPH in ethanol and the mixture was taken under vigorous stirring at room temperature. After 10 min, the solution was filtered and absorbance at 515 nm was measured by UV/vis measurements using a Hp 8453 UV-spectrophotometer. Results were expressed as percentage of reduction of the initial DPPH radical absorption. Experiments were run in triplicate.

2,2′-Azinobis(3-ethylbenzothiazoline-6-sulfonic acid) (ABTS) Assay. The ABTS radical cation ($ABTS^{\bullet+}$) was produced as described[53] by reacting ABTS with potassium persulfate. The $ABTS^{\bullet+}$ solution was diluted with ethanol to an absorbance of 0.70 at 745 nm. Mel-TOCNF or blank TOCNF aerogels were finely cut with scissors and suspended at 0.5−1.5 mg mL^{-1} in this solution. The mixture was taken under vigorous stirring at room temperature, and after 10 min the absorbance at 745 nm was measured. Results were

DOI: 10.1021/acs.biomac.5b01497
Biomacromolecules XXXX, XXX, XXX−XXX

expressed as percentage of reduction of the initial $ABTS^{\bullet+}$ absorption. Experiments were run in triplicate.

Adsorption Experiments. *Methylene Blue (MB) Adsorption Studies:*[27] Adsorption experiments were performed at room temperature by immersion of Mel-TOCNF or blank TOCNF aerogels (58 mg average) in a 2 mg L^{-1} MB ethanolic solution (10 mL). At different time-points, the liquid was sampled (5 mL), immediately centrifuged (2 min, 1000 rpm), and the absorbance at 654 nm of the supernatant measured by UV/vis measurements using a Beckman DU640 UV-spectrophotometer. After the measurement, the liquid was remixed with the fraction containing the solid and added to the original suspension. Results were expressed as percentage of reduction of the initial MB absorption. Experiments were run in triplicate. Other experiments were performed on TOCNF aerogels finely cut with scissors and under magnetic stirring.

RESULTS AND DISCUSSION

Synthesis and Characterization of Eumelanin-Coated Aerogels. Cellulose aerogels were prepared according to an optimized procedure previously reported[21,27] and described in detail in the Materials and Methods. TOCNF were first obtained by TEMPO/NaClO-mediated oxidation of cotton cellulose. The protocol consists of the selective conversion of a variable amount of C6 hydroxyl functional moieties of cotton cellulose backbone to the corresponding carboxylic groups (Scheme 1, path a). Titration revealed a content of carboxylic acid units of 1.1 mmol g^{-1}.[21]

By operating under basic conditions, it is possible to promote defibrillation of cellulose, thanks to the electrostatic repulsion of the negative charges distributed on the nanofibers (Scheme 1, path b), while following acidification allows the recovery of cellulose nanofibers (Scheme 1, path c).

Milky suspensions of so-prepared TOCNF were pipetted in 24-well plates and frozen at −80 °C. The subsequent freeze-drying at −60 °C for 2 days afforded white cylindrical TOCNF-aerogels with a final volume of 7 cm^3, a bulk density d_b of about 40 mg cm^{-3}, and a resulting porosity of 97.5%. TOCNF-aerogels thus prepared were coated with eumelanin using the recently developed AISSP[41] of DHI (Scheme 2) and DHICA. Figure 2 shows complete aerogel coating, as apparent from the dark colorations, black in the case of DHI, or dark brown in the case of DHICA.

The ^{13}C cross-polarization-magic angle spinning (CP-MAS) solid state NMR spectrum of dried DHI Mel-TOCNF aerogel is reported in Figure 3. In addition to the peaks associated with the carbons of the anhydroglucose units of cellulose,[54] and the signal at 175 ppm, which should be ascribed to the carboxylic groups deriving from the oxidation of pristine polysaccharide,[21] a broad signal appearing at 130−140 ppm reveals the presence of aromatic carbons, which can be uniquely ascribed to DHI units on the material surface. As DHI and DHICA melanins are characterized by the presence of unpaired electrons, which are easily detected by electron paramagnetic resonance (EPR) spectroscopy,[32,46] with the aim to further confirm the formation of a melanin coating on the TOCNF surface and to characterize its structural features, EPR measurements were carried out on DHI Mel-TOCNF and DHICA Mel-TOCNF samples.

Scheme 2. Schematic Illustration of AISSP DHI-Coating of White TOCNF-Aerogels (DHICA Coating is Not Shown)

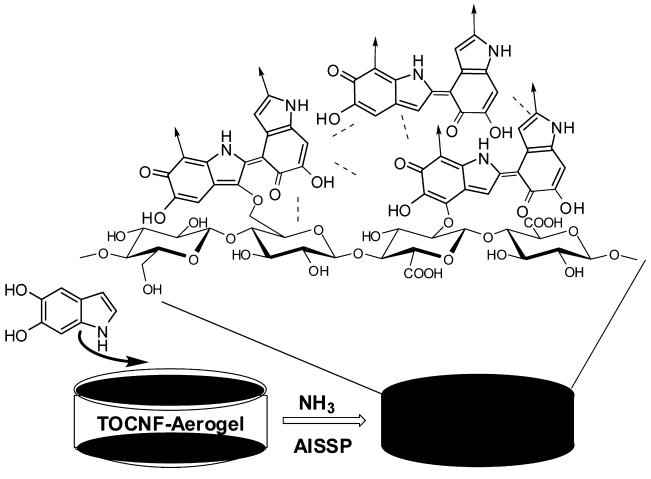

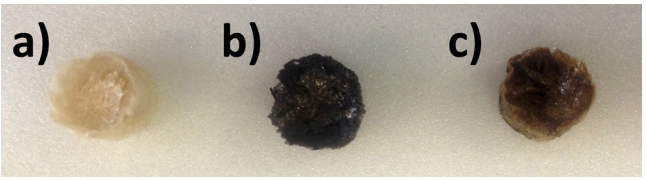

Figure 2. (a) TOCNF (untreated), (b) DHI Mel-TOCNF, and (c) DHICA Mel-TOCNF aerogels.

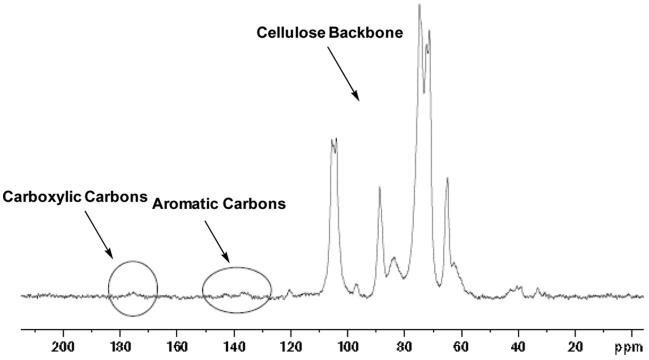

Figure 3. ^{13}C CP-MAS solid state NMR spectrum of dried DHI Mel-TOCNF aerogel.

In the former case a well-detectable single peak is obtained (Figure 4a), while in the latter one a very weak and broad signal is observed. For comparison, the EPR spectra of DHI and DHICA melanin obtained by the same synthetic protocol were registered. The DHI Mel-TOCNF and DHI melanin spectra are very similar, as quantitatively confirmed by the signal amplitude ΔB (5.7 ± 0.3 vs 5.3 ± 0.2) and the g value (2.0029 ± 0.0003 vs 2.0030 ± 0.0002), which is consistent with the presence of carbon-centered radicals.[46]

Moreover, the normalized power saturation profiles, reported in Figure 4b, show for both samples a maximum after which only a limited intensity decrease is observed, suggesting a quite heterogeneous distribution of the radical centers. These evidence indicate that the coating on the TOCNF surface presents the same features of pure DHI melanin. Based on the spin density determined for DHI melanin (~7×10^{18} spin g^{-1}), a semiquantitative estimation of the melanin weight fraction in the DHI Mel-TOCNF sample indicates a value of about 1×10^{-3}. In the case of DHICA Mel-TOCNF, the comparison with the DHICA melanin spectrum shows that the degree of deposition of the melanin coating is very limited, thus hampering a detailed analysis of the spectral features.

DOI: 10.1021/acs.biomac.5b01497
Biomacromolecules XXXX, XXX, XXX−XXX

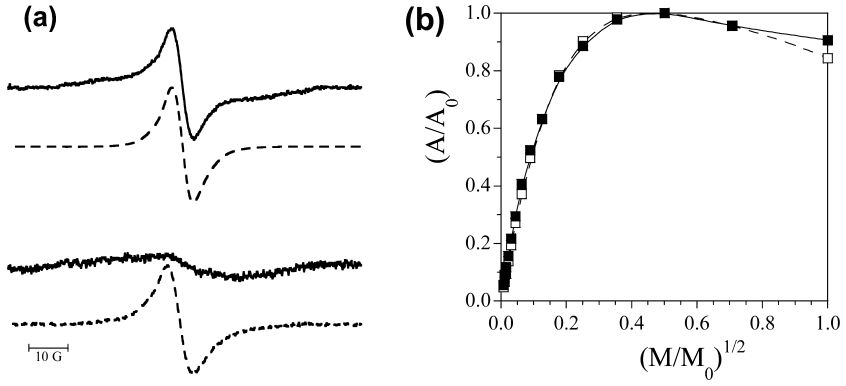

Figure 4. (a) EPR spectra of DHI Mel-TOCNF and DHI melanin (upper part of the figure, continuous and dashed line, respectively) and DHICA Mel-TOCNF and DHICA melanin (lower part of the figure, continuous and dashed line, respectively) samples. DHI Mel-TOCNF and DHICA Mel-TOCNF spectra have been normalized by the sample weight. (b) Amplitude vs power intensities of DHI Mel-TOCNF (full squares) and DHI melanin (open squares).

Both Mel-TOCNF aerogels resulted stable at acidic conditions, but not under basic ones. Similarly to uncoated TOCNF, the melanin coated nanofibers of Mel-TOCNF are completely dispersed in water at pH ≈12, as can be clearly seen in Figure 5, which refers to DHI Mel-TOCNF. The aqueous

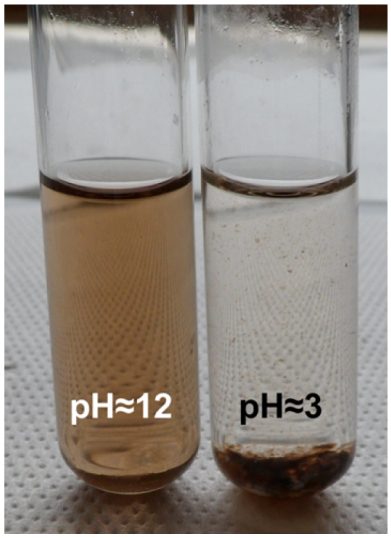

Figure 5. Effect of pH on DHI Mel-TOCNF stability.

phase assumes the characteristic brown color of the melanin pigments. After acidification (pH < 5), Mel-TOCNF aggregates together precipitating at the bottom of the flask. The aqueous phase is completely transparent, indicating no DHI release in solution.

Finally, scanning electron microscopy (SEM) analysis (Figure 6) showed that the pristine porous architecture of CNF-aerogels was virtually unaffected by eumelanin coating, confirming that the polymerization process occurred on the template surface, without forming lumps or occluding the pores. The 2D-sheet like morphology of the pore walls, usually observed for CNF-aerogels obtained from the freeze-drying of aqueous suspensions with a content of dry cellulose higher than 0.5% w/v,[50] is preserved after the induced polymerization. At higher magnification, the polymer deposition is manifested, appearing to be more significant for DHI Mel-TOCNF aerogels, compared to DHICA Mel-TOCNF ones. SEM images were also obtained from cryo-sectioned samples (Figure S1,

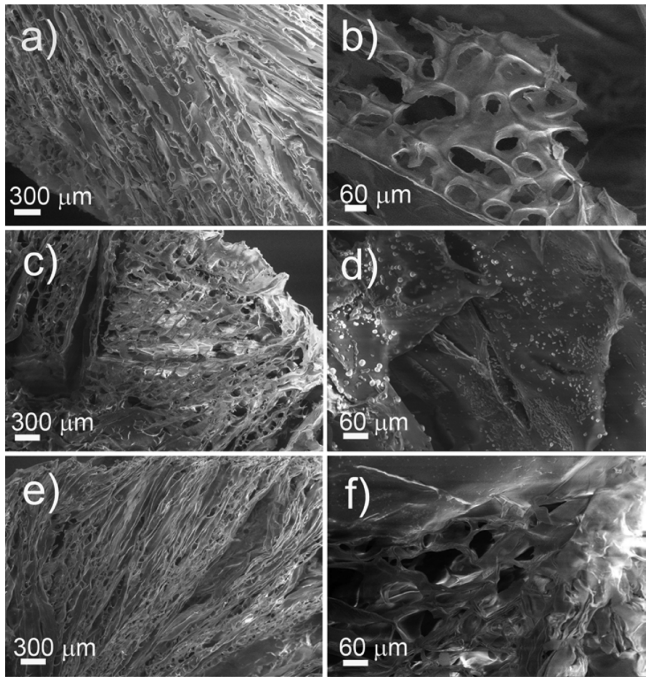

Figure 6. SEM images of (a, b) TOCNF, (c, d) DHI Mel-TOCNF, and (e, f) DHICA Mel-TOCNF aerogels.

Supporting Information), evidencing the uniformity and the thicknesses of the coating.

The higher efficiency in DHI coating also resulted in a significant modification of the surface wetting property of the aerogel, as confirmed by water contact angle (WCA) measurements. As expected due to its hydrophilic surface, TOCNF aerogel adsorbed the water droplets instantaneously (Movie S1, Supporting Information). A slightly slower, but still very fast water adsorption was observed for the DHICA Mel-TOCNF aerogel as well (Movie S2, Supporting Information). For both these two materials, it was impossible to measure any WCA. On the contrary, the DHI Mel-TOCNF aerogel showed a higher hydrophobicity (Movie S3, Supporting Information), with a WCA of 94.2° (Figure 7).

Antioxidant Assays. The antioxidant capacity of Mel-TOCNF aerogels was assessed through the 2,2-diphenyl-1-picrylhydrazyl (DPPH)[51,52] and 2,2′-azinobis(3-ethylbenzothiazoline-6-sulfonic acid) (ABTS)[53] assays. DPPH is a stable free

DOI: 10.1021/acs.biomac.5b01497
Biomacromolecules XXXX, XXX, XXX−XXX

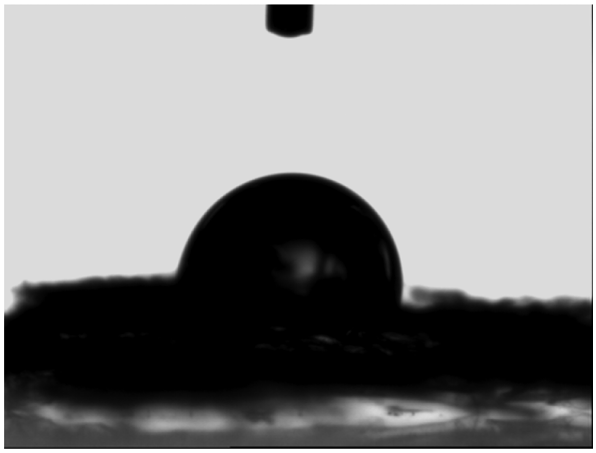

Figure 7. WCA on DHI Mel-TOCNF aerogel.

radical characterized by a strong absorption maximum at 515 nm and a deep violet color in ethanol solution. Upon interaction with a reducing agent, DPPH turns into a yellow hydrazine, which has no absorption in the visible region (Figure 8a). By monitoring the decrease of the absorption at 515 nm of a solution of DPPH in the presence and in the absence of an antioxidant, it is possible to estimate the reducing activity of the latter. ABTS radical cation, which is produced by oxidation of ABTS with potassium persulfate prior to the addition of antioxidant, has a blue-green chromophore absorption and the antioxidant activity is determined by its decolorization, by measuring the reduction of the radical cation as the percentage inhibition of absorbance at 734 nm.

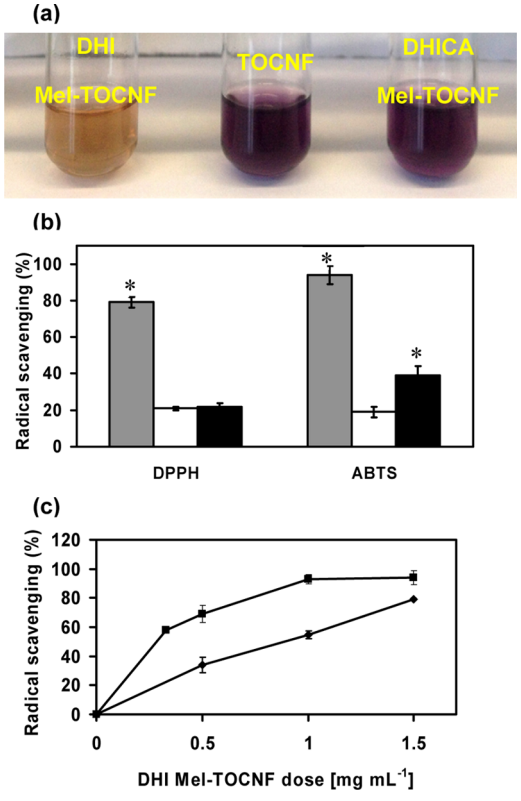

Figure 8. (a) DPPH reduction by TOCNF and Mel-TOCNF-aerogels (1.5 mg mL^{-1}). (b) Free radical scavenging properties of DHI Mel-TOCNF (gray bars), TOCNF (white bars), and DHICA Mel-TOCNF (black bars) aerogels at 1.5 mg mL^{-1} (mean values ± SD, n = 3 experiments). *P < 0.05 with respect to TOCNF. (c) Free radical scavenging by DHI Mel-TOCNF aerogel at different doses (mean values ± SD, n = 3 experiments): (▲) DPPH assay; (■) ABTS assay.

The results reported in Figure 8b show very good reducing properties in both assays for the DHI Mel-TOCNF aerogel compared to the blank TOCNF aerogel. The low antioxidant activity exhibited by the DHICA Mel-TOCNF aerogel can be ascribed to the lower degree of melanization achieved with the less oxidizable melanin precursor DHICA, as observed by SEM and EPR analysis. Figure 8c shows that the free radical scavenging by DHI Mel-TOCNF increases by increasing the amount of solid in suspension.

Methylene Blue (MB) Adsorption Test. Figure 9 reports the results of MB adsorption test performed on the Mel-TOCNF aerogels in comparison to the blank TOCNF sample, following a protocol previously reported.[27] DHI melanin-coating significantly improved the adsorption capacity of TOCNF aerogels leading to 35% adsorption after 3 h vs 15% adsorption observed for the blank sample. Conversely, no significant difference in the adsorption properties were observed comparing the DHICA Mel-TOCNF aerogel with the blank. A considerable improvement in the adsorbent capacity was achieved by finely dispersing the aerogels in the MB solution (particle sizes of 2−3 mm), especially in the case of the DHICA Mel-CNF aerogel. Notably, DHI melanin prepared by the AISSP protocol did not show significant adsorption capacity toward MB, indicating that deposition onto the nanocellulose template is critical for this capacity (data not shown).

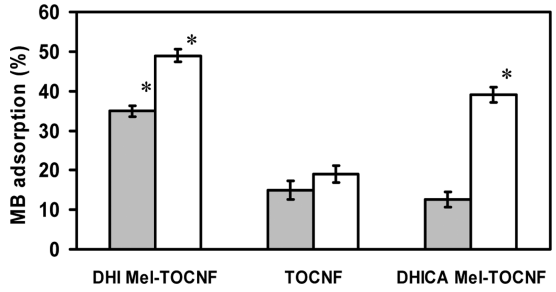

Figure 9. MB adsorption by TOCNF aerogels as circular disks (gray bars) or fine dispersion (white bars). *P < 0.05 with respect to TOCNF.

CONCLUSIONS

An all-natural aerogel with a multifunctional eumelanin coating has been prepared from cellulose nanofibers (CNF) by a recently developed procedure involving ammonia-induced solid state polymerization (AISSP) of suitable melanogenic precursors, that is, 5,6-dihydroxyindole (DHI) or 5,6-dihydroxyindole-2-carboxylic acid (DHICA). The resulting highly porous organic aerogels exhibited structural and paramagnetic properties compatible with an inner cellulose template covered by a eumelanin-like coating, conferring potent antioxidant activity and strong adsorption capacity toward organic dyes. Both the properties of the new multifunctional aerogels and the scope of the expedient synthetic protocol used for their preparation are worthy of further investigations for application in a range of biomedical and technological sectors.

DOI: 10.1021/acs.biomac.5b01497
Biomacromolecules XXXX, XXX, XXX−XXX

■ ASSOCIATED CONTENT

Supporting Information

The Supporting Information is available free of charge on the ACS Publications website at DOI: 10.1021/acs.biomac.5b01497.

Movie S1, WCA determination (AVI).
Movie S2, WCA determination (AVI).
Movie S3, WCA determination (AVI).
Figure S1, reporting sectioned samples of coated aerogels (PDF).

■ AUTHOR INFORMATION

Corresponding Authors

*E-mail: panzella@unina.it.
*E-mail: carlo.punta@polimi.it.

Notes

The authors declare no competing financial interest.

■ ACKNOWLEDGMENTS

We are grateful to Enrico Caneva (Centro Interdipartimentale Grandi Apparecchiature-CIGA, University of Milan, Italy) for ^{13}C CP-MAS NMR spectra. Italian MIUR (PRIN 2010-2011, PROxi Project 2010PFLRJR_005) and Regione Toscana (POR FESR 2014-2020, Call RSI 2014, Project NanoBonD) are acknowledged for financial support

■ REFERENCES

(1) Hüsing, N.; Schubert, U. *Angew. Chem.* **1998**, *110*, 22−47; *Angew. Chem., Int. Ed.* **1998**, *37*, 22−45.
(2) Pierre, A. C.; Pajonk, G. M. *Chem. Rev.* **2002**, *102*, 4243−4266.
(3) Gesser, H. D.; Goswami, P. C. *Chem. Rev.* **1989**, *89*, 765−788.
(4) Pekala, R. W. *J. Mater. Sci.* **1989**, *24*, 3221−3227.
(5) Leventis, N. *Acc. Chem. Res.* **2007**, *40*, 874−884.
(6) Boday, D. J.; Keng, P. Y.; Muriithi, B.; Pyun, J.; Loy, D. A. *J. Mater. Chem.* **2010**, *20*, 6863−6865.
(7) Moon, R. J.; Martini, A.; Nairn, J.; Simonsen, J.; Youngblood, J. *Chem. Soc. Rev.* **2011**, *40*, 3941−3994.
(8) Chen, W.; Li, Q.; Wang, Y.; Yi, X.; Zeng, J.; Yu, H.; Liu, Y.; Li, J. *ChemSusChem* **2014**, *7*, 154−161.
(9) Siró, I.; Plackett, D. *Cellulose* **2010**, *17*, 459−494.
(10) Jiang, F.; Hsieh, Y.-L. *J. Mater. Chem. A* **2014**, *2*, 6337−6342.
(11) Isogai, A.; Saito, T.; Fukuzumi, H. *Nanoscale* **2011**, *3*, 71−85.
(12) Biliuta, G.; Fras, L.; Drobota, M.; Persin, Z.; Kreze, T.; Stana-Kleinschek, K.; Ribitsch, V.; Harabagiu, V.; Coseri, S. *Carbohydr. Polym.* **2013**, *91*, 502−507.
(13) Coseri, S.; Biliuta, G.; Simionescu, B. C.; Stana-Kleinschek, K.; Ribitsch, V.; Harabagiu, V. *Carbohydr. Polym.* **2013**, *93*, 207−215.
(14) Jiang, F.; Hsieh, Y.-L. *J. Mater. Chem. A* **2014**, *2*, 350−359.
(15) Kobayashi, Y.; Saito, T.; Isogai, A. *Angew. Chem.* **2014**, *126*, 10562−10565; *Angew. Chem., Int. Ed.* **2014**, *53*, 10394−10397.
(16) Shimotoyodome, A.; Suzuki, J.; Kumamoto, Y.; Hase, T.; Isogai, A. *Biomacromolecules* **2011**, *12*, 3812−3818.
(17) Dong, H.; Snyder, J. F.; Williams, K. S.; Andzelm, J. W. *Biomacromolecules* **2013**, *14*, 3338−3345.
(18) Petersen, N.; Gatenholm, P. *Appl. Microbiol. Biotechnol.* **2011**, *91*, 1277−1286.
(19) Yang, X.; Cranston, E. D. *Chem. Mater.* **2014**, *26*, 6016−6025.
(20) Mueller, S.; Sapkota, J.; Nicharat, A.; Zimmermann, T.; Tingaut, P.; Weder, C.; Foster, E. J. *J. Appl. Polym. Sci.* **2015**, *132*, 41740−41753.
(21) Melone, L.; Rossi, B.; Pastori, N.; Panzeri, W.; Mele, A.; Punta, C. *ChemPlusChem* **2015**, *80*, 1408−1415.
(22) Melone, L.; Bonafede, S.; Tushi, D.; Punta, C.; Cametti, M. *RSC Adv.* **2015**, *5*, 83197−83205.
(23) Olsson, R. T.; Samir, M.; Salazar-Alvarez, G.; Belova, L.; Strom, V.; Berglund, L. A.; Ikkala, O.; Nogues, J.; Gedde, U. W. *Nat. Nanotechnol.* **2010**, *5*, 584−588.
(24) Aulin, C.; Netrval, J.; Wagberg, L.; Lindstrom, T. *Soft Matter* **2010**, *6*, 3298−3305.
(25) Kettunen, M.; Silvennoinen, R. J.; Houbenov, N.; Nykanen, A.; Ruokolainen, J.; Sainio, J.; Pore, V.; Kemell, M.; Ankerfors, M.; Lindstrom, T.; Ritala, M.; Ras, R. H. A.; Ikkala, O. *Adv. Funct. Mater.* **2011**, *21*, 510−517.
(26) Korhonen, J. T.; Hiekkataipale, P.; Malm, J.; Karppinen, M.; Ikkala, O.; Ras, R. H. A. *ACS Nano* **2011**, *5*, 1967.
(27) Melone, L.; Altomare, L.; Alfieri, I.; Lorenzi, A.; De Nardo, L.; Punta, C. *J. Photochem. Photobiol., A* **2013**, *261*, 53−60.
(28) Simon, J. D.; Peles, D.; Wakamatsu, K.; Ito, S. *Pigm. Cell Melanoma Res.* **2009**, *22*, 563−579.
(29) Simon, J. D.; Peles, D. *Acc. Chem. Res.* **2010**, *43*, 1452−1460.
(30) Ito, S.; Wakamatsu, K.; d'Ischia, M.; Napolitano, A.; Pezzella, A. Structure of Melanins. In *Melanins and Melanosomes*; Borovanský, J., Riley, P. A., Eds.; Wiley-VCH: Weinheim, 2011; pp 167−185.
(31) d'Ischia, M.; Napolitano, A.; Pezzella, A.; Meredith, P.; Sarna, T. *Angew. Chem.* **2009**, *121*, 3972−3979; *Angew. Chem., Int. Ed.* **2009**, *48*, 3914−3921.
(32) Panzella, L.; Gentile, G.; D'Errico, G.; Della Vecchia, N. F.; Errico, M. E.; Napolitano, A.; Carfagna, C.; d'Ischia, M. *Angew. Chem.* **2013**, *125*, 12916−12919; *Angew. Chem., Int. Ed.* **2013**, *52*, 12684−12687.
(33) Liu, Y.; Ai, K.; Lu, L. *Chem. Rev.* **2014**, *114*, 5057−5115.
(34) Lee, H.; Dellatore, S. M.; Miller, W. M.; Messersmith, P. B. *Science* **2007**, *318*, 426−430.
(35) Sedó, J.; Saiz-Poseu, J.; Busqué, F.; Ruiz-Molina, D. *Adv. Mater.* **2013**, *25*, 653−701.
(36) Kang, S. M.; Hwang, N. S.; Yeom, J.; Park, S. Y.; Messersmith, P. B.; Choi, I. S.; Langer, R.; Anderson, D. G.; Lee, H. *Adv. Funct. Mater.* **2012**, *22*, 2949−2955.
(37) Waite, J. H. *Nat. Mater.* **2008**, *7*, 8−9.
(38) Dreyer, D. R.; Miller, D. J.; Freeman, B. D.; Paul, D. R.; Bielawski, C. W. *Chem. Sci.* **2013**, *4*, 3796−3802.
(39) Lynge, M. E.; van der Westen, R.; Postma, A.; Städler, B. *Nanoscale* **2011**, *3*, 4916−4928.
(40) Xu, Q.; Kong, Q.; Liu, Z.; Zhang, J.; Wang, X.; Liu, R.; Yuea, L.; Cui, G. *RSC Adv.* **2014**, *4*, 7845−7850.
(41) Pezzella, A.; Barra, M.; Musto, A.; Navarra, A.; Alfè, M.; Manini, P.; Parisi, S.; Cassinese, A.; Criscuolo, V.; d'Ischia, M. *Mater. Horiz.* **2015**, *2*, 212−220.
(42) Bonadies, I.; Cimino, F.; Carfagna, C.; Pezzella, A. *Biomacromolecules* **2015**, *16*, 1667−1670.
(43) d'Ischia, M.; Napolitano, A.; Ball, V.; Chen, C.-T.; Buehler, M. J. *Acc. Chem. Res.* **2014**, *47*, 3541−3550.
(44) Pezzella, A.; Crescenzi, O.; Panzella, L.; Napolitano, A.; Land, E.; Barone, V.; d'Ischia, M. *J. Am. Chem. Soc.* **2013**, *135*, 12142−12149.
(45) d'Ischia, M.; Wakamatsu, K.; Napolitano, A.; Briganti, S.; Garcia-Borron, J.-C.; Kovacs, D.; Meredith, P.; Pezzella, A.; Picardo, M.; Sarna, T.; Simon, J. D.; Ito, S. *Pigm. Cell Melanoma Res.* **2013**, *26*, 616−633.
(46) Mostert, A. B.; Hanson, G. R.; Sarna, T.; Gentle, I. R.; Powell, B. J.; Meredith, P. *J. Phys. Chem. B* **2013**, *117*, 4965−4972.
(47) Edge, R.; d'Ischia, M.; Land, E. J.; Napolitano, A.; Navaratnam, S.; Panzella, L.; Pezzella, A.; Ramsden, C. A.; Riley, P. A. *Pigm. Cell Res.* **2006**, *19*, 443−450.
(48) Cesareo, E.; Korkina, L.; D'Errico, G.; Vitiello, G.; Aguzzi, M. S.; Passarelli, F.; Pedersen, J. Z.; Facchiano, A. *PLoS One* **2012**, *7*, e48849.
(49) Yordanova, V. N.; Gancheva, V.; Pelova, V. A. *J. Radioanal. Nucl. Chem.* **1999**, *240*, 619−622.
(50) Chen, W.; Yu, H.; Li, Q.; Liu, Y.; Li, J. *Soft Matter* **2011**, *7*, 10360−10368.
(51) Goupy, P.; Dufour, C.; Loonis, M.; Dangles, O. *J. Agric. Food Chem.* **2003**, *51*, 615−622.
(52) Gökmen, V.; Serpen, A.; Fogliano, V. *Trends Food Sci. Technol.* **2009**, *20*, 278−288.

DOI: 10.1021/acs.biomac.5b01497
Biomacromolecules XXXX, XXX, XXX−XXX

(53) Re, R.; Pellegrini, N.; Proteggente, A.; Pannala, A.; Yang, M.; Rice-Evans, C. *Free Radical Biol. Med.* **1999**, *26*, 1231−1237.
(54) Vismara, E.; Melone, L.; Gastaldi, G.; Cosentino, C.; Torri, G. *J. Hazard. Mater.* **2009**, *170*, 798−808.

DOI: 10.1021/acs.biomac.5b01497
Biomacromolecules XXXX, XXX, XXX−XXX